# LoRea: A Backscatter Architecture that Achieves a Long Communication Range

Ambuj Varshney
Uppsala University
Sweden
ambuj.varshney@it.uu.se

Oliver Harms
Uppsala University
Sweden
mail@oliverharms.eu

Carlos Pérez-Penichet
Uppsala University
Sweden
carlos.penichet@it.uu.se

Christian Rohner
Uppsala University
Sweden
christian.rohner@it.uu.se

Frederik Hermans
Uppsala University
Sweden
frederik@it.uu.se

Thiemo Voigt
Uppsala University and RISE SICS
Sweden
thiemo@sics.se

## ABSTRACT

There is the long-standing assumption that radio communication in the range of hundreds of meters needs to consume mWs of power at the transmitting device. In this paper, we demonstrate that this is not necessarily the case for some devices equipped with backscatter radios. We present LoRea an architecture consisting of a tag, a reader and multiple carrier generators that overcomes the power, cost and range limitations of existing systems such as Computational Radio Frequency Identification (CRFID). LoRea achieves this by: *First*, generating narrow-band backscatter transmissions that improve receiver sensitivity. *Second*, mitigating self-interference without the complex designs employed on RFID readers by keeping carrier signal and backscattered signal apart in frequency. *Finally*, decoupling carrier generation from the reader and using devices such as WiFi routers and sensor nodes as a source of the carrier signal. An off-the-shelf implementation of LoRea costs 70 USD, a drastic reduction in price considering commercial RFID readers cost 2000 USD. LoRea's range scales with the carrier strength, and proximity to the carrier source and achieves a maximum range of 3.4 km when the tag is located at 1 m distance from a 28 dBm carrier source while consuming 70 µW at the tag. When the tag is equidistant from the carrier source and the receiver, we can communicate upto 75 m, a significant improvement over existing RFID readers.

## KEYWORDS

Battery-free, Backscatter, CRFIDs, WISP, Moo, Ultra-low power, long range communication, RFIDs

## 1 INTRODUCTION

Backscatter communication enables wireless transmissions at a power consumption orders of magnitude lower than traditional radios. A backscatter transmitter modulates ambient wireless signals by selectively reflecting or absorbing them, which consumes less than 1 µW of power [37]. This makes backscatter communications well-suited for applications where replacing batteries is challenging [42, 69] or where extending battery life is important [27]. In the past few years, significant progress has been made to advance backscatter communication. Recent works demonstrate the ability to synthesise transmissions compatible with WiFi (802.11b) [33], BLE [22] and ZigBee [30, 51] at µWs of power using backscatter transmissions. Other works leverage ambient wireless signals like television [37, 50] or WiFi [32, 71, 73] for communication. On the other hand, the design of traditional backscatter readers and tags, e.g., CRFID systems, has not seen major improvements despite their continuing significance [18, 26, 42, 58, 70] and the widespread deployment of passive RFID systems.

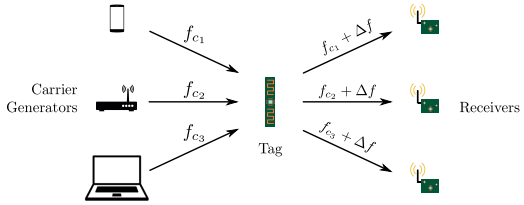


**Figure 1:** *Overview of our architecture.* One or more devices (sensor nodes, WiFi access points, etc.) provide the carrier signal that the backscatter tag reflects to transmit. The backscattered signal is received by one or more receivers.

Existing CRFIDs, like WISP [55] and Moo [72], augment traditional RFID tags with sensing and computational capabilities [10]. These tags operate on harvested energy and, over the years, have been used to prototype many applications such as localisation [75], wireless microphones [57] or infrastructure monitoring [20]. Many of these applications require a large communication range, e.g., battery-free cameras [42], but are restricted to operate at very short range (few meters) due to the limited range achievable with existing RFID readers. Further, these applications are also constrained by the high cost ( $\geq$ \$2000) and power consumption of the readers.

To understand the reason for the poor performance of existing CRFID systems, we see how these systems operate: CRFID tags require an external device (the reader) that generates a carrier signal, provides power, queries and receives the backscatter reflections from the tags. In most CRFID readers, a single device performs all of these operations. The readers receive backscatter transmissions at the frequency of the carrier signal [11, 26, 28, 67, 74]. As


*SenSys '17, Delft, Netherlands*
 978-1-4503-5459-2/17/11…$15.00
DOI: 10.1145/3131672.3131691

| System name | LoRea-868 | LoRea-2.4 | Passive WiFi [33] | HitchHike [73] | InterScatter [30] | BLE [22] | BackFi [6] | RFID [28] |
|---|---|---|---|---|---|---|---|---|
| **Carrier strength (dBm)** | 28 | 26 | 30 | 30 | 20 | 15 | 30 | 31.5 |
| **Reported range (m)** | 3400 | 225/175 | 33 | 54 | 10 | 9.5 | 5 | >10 |
| **Bitrate (kbps)** | 2.9 | 2.9/197 | 1000/11000 | 222 | 1000/11000 | 1000 | 1000 | 640 |
| **Tag power consumption** | 70 µW | 650 µW | 14.5 µW (1 Mbps)<br>59.2 µW (11 Mbps) | 33 µW | 28 µW | N.A | N.A | 30 µW |

**Table 1: Comparison of LoRea with backscatter systems which consume µWs of power for transmissions. LoRea's tag was located at a distance of 1 m from the carrier generator, similar to all the other systems. Reported ranges are line-of-sight.**

energy delivery is combined with communication, the readers generate a strong carrier signal (~ 30 dBm/ 1 W), which significantly increases their power consumption making applications such as mobile backscatter readers very challenging to achieve (see Section 5.1). The backscatter reflections, are inherently weak, hence separating them from the strong carrier requires complex techniques which increases both cost and complexity [27]. The readers also suffer from poor sensitivity (-84 dBm [28]) due to leakage of the carrier signal into the receive path [39].

An inexpensive backscatter platform that achieves high communication range could significantly help applications conceived using CRFIDs. Further, such a platform could enable new battery-free applications that are extremely challenging right now. For example, sensors embedded within the infrastructure (see Section 5.2). We present an architecture that attempts to enable such capability.

**Contributions.** We redesign CRFID-based systems and introduce a new architecture shown in Figure 1. We achieve a significant improvement across key metrics like range, price and power consumption in comparison to the state of the art [6, 22, 30, 33, 73]. Our architecture is based on the following design elements:

(1) The tradeoff between bitrate and receiver sensitivity is well known. Recent state-of-the-art- and ultra-low-power backscatter systems operate at high bitrates (thousands of kilobit/s) due to the use of commodity protocols [6, 22, 30, 33, 73] which limits their range and applicability. We deliberately operate at low bitrates (2.9 kbit/s) which allows us to use highly sensitive narrow-band receivers. Such a design is not detrimental to most sensing applications as they only send small amounts of information [47].
(2) We keep the carrier and backscattered signals at different frequencies. This improves the SNR of the backscattered signal (see Section 2) by reducing the interference from the carrier signal. As opposed to traditional readers that use complex solutions to reduce self-interference, our architecture leverages the ability of commodity transceivers to reject emissions on adjacent channels.
(3) Finally, we use a bistatic configuration where the carrier generator and the receiver are spatially separated. This has three advantages: First, spatial separation decreases self-interference which improves the range owing to pathloss of the carrier signal. Second, when operating in the 2.4 GHz band, we can leverage commodity devices to provide the carrier signal. Third, decoupling helps to separate the energy-intensive carrier generation from the reader.

In our architecture, the communication range scales with the strength of the carrier signal and the proximity of the tag to the carrier source. This property is inherent in state-of-the-art backscatter systems [30, 33]. When operating in close proximity (1 m), and with the strength of the carrier signal close to the maximum permissible power, we achieve a range of more than 3.4 km in the 868 MHz band, and 225 m in the 2.4 GHz band with a carrier strength of 28 dBm and 26 dBm respectively. This range is an order of magnitude longer than what state-of-the-art systems achieve [30, 33, 73] when operating in similar settings (see Table 1). When the tag is located equidistant from both the carrier source and the receiver, a scenario that encounters path loss similar to monostatic RFID readers, we achieve a range of 75 m, a significant improvement in range over traditional CRFID readers.

Design elements (2) and (3) have also been used in recent backscatter systems [30, 33, 73]. Combining the three design elements enables us to significantly reduce self-interference without using the complex designs employed by current CRFID readers. This helps us to reduce the price of the reader to 70 USD, a drastic reduction when compared with the approx. 2000 USD that commercial RFID readers cost (see Section 3.5).

Finally, design element (3) enables us to use an infrastructure of wireless devices as the source of the unmodulated carrier signal. This reduces the power consumption of the reader, as the carrier generation is the most energy intensive operation in backscatter readers. While Interscatter [30] demonstrated that BLE radios can be used to generate unmodulated carrier signals, we go a step beyond and demonstrate that 802.15.4 and WiFi radios can also generate carrier signals, which makes it possible to delegate the energy expensive carrier generation to mains-powered devices like WiFi routers or ZigBee hubs (see Section 3.2.3).

Keeping the carrier and backscatter signal separated in frequency, also introduces a new challenge in the design of the tag. Traditional CRFID tags only modulate the carrier with information while our architecture requires the carrier to be frequency-shifted and modulated. Recent low-power designs of such tags are implemented on ASICs and are in simulations [30, 33, 68], or designs built using off-the-shelf components modulate ambient signals to amplitude modulated signal [71]. We present a backscatter tag that can shift and frequency modulate the carrier signal. The tag consumes 70 µW and 650 µW while operating at 868 MHz and 2.4 GHz respectively.

In using commodity devices as carrier generators, our architecture operates in the shared 2.4 GHz ISM band and encounters the problem of cross-technology interference (CTI). To mitigate the harmful effects of CTI, we demonstrate two mechanisms: First, we show that leveraging multiple wireless devices to generate carrier signals at different frequencies can enable simultaneous backscatter transmissions. When coupled with several receivers the probability of reception improves, even under CTI. Second, our results demonstrate that by changing the frequency of the carrier signal, we can make backscatter transmissions avoid CTI.

Note that in our use cases, as well as in the rest of the paper, we focus on the uplink from the backscatter tag to the reader since most

sensing applications are constrained by this link [6, 73]. We can support receptions using existing low-power receiver designs [32]. Existing CRFID readers combine energy delivery with communication on the same RF carrier, which has been shown to be inefficient [24, 70]. We hence decouple the RF energy delivery from the reader. Our backscatter tag still consumes μWs, which can be easily provided by many ambient energy sources [8]. Further, LoRea, if needed, can support RF-based energy harvesting by using the harvester design presented by Talla et al. [56].

The paper proceeds as follows. We discuss background and related work in Section 2. Next, we discuss the design, implementation and cost analysis of our architecture in Section 3. In Section 4 we present our experimental evaluation. Section 5 discusses two challenging applications our architecture enables. Before concluding, we discuss some issues related to our architecture in Section 6.

## 2 BACKGROUND AND STATE OF THE ART

This section presents a background on backscatter and self-interference as well as work related to LoRea.

### 2.1 Backscatter primer

**Overview.** When radio frequency (RF) signals interact with an antenna, they are absorbed or reflected by a varying amount dictated by the antenna's radar cross section (RCS). Backscatter devices control the RCS by changing the impedance of the circuit connected to the antenna, switching the antenna to either reflecting or absorbing mode. This mode change induces minute variations in the ambient signal which can be observed by an RF receiver.

Consider an RF emitter that is transmitting a signal $S_{rt}(t)$ that reaches the antenna of the backscatter device. The device selectively reflects or absorbs $S_{rt}(t)$. At a receiver, the reflected signal $R(t)$ consists of two components: $S_{rt}(t)$ coming directly from the emitter device and $S_{bt}(t)$ caused by the minute variations induced by the backscatter operation. The resulting signal can be expressed as:

$$R(t) = S_{rt}(t) + \sigma B(t) S_{bt}(t) \quad (1)$$

In the above equation, $\sigma$ is the RCS of the device, and $B(t)$ is the bit sequence transmitted by the device, that is 1 when reflecting, and 0 when absorbing. In traditional RFID readers, the reader both generates the carrier signal and receives the backscattered signal. The reader generates a tone signal or a pure sinusoid at frequency $f_c$, and the backscatter tag reflects at the same frequency, i.e., in the above equation both components are at the same frequency.

**Backscatter as mixing process.** Equation (1) shows that the signal backscattered from the tag is proportional to the product of the baseband signal $B(t)$ generated by the tag and the ambient signal $S_{bt}(t)$ at the tag. If we assume that backscatter readers generate a carrier signal at a specific frequency $f_c$, while the tag is changing the RCS of the antenna at a frequency of $\Delta f$, the resulting signal (product $\sigma B(t) S_{bt}(t)$ in Equation 1) can be expanded to the following form:

$$2\sin(f_c t)\sin(\Delta f t) = \cos[(f_c + \Delta f)t] - \cos[(f_c - \Delta f)t]. \quad (2)$$

The result is that the backscattered signal appears at an offset $\Delta f$ on the positive and the negative sides of $f_c$, the centre of the carrier signal. This displacement helps the backscatter tag both modulate the carrier and reduce interference from the carrier to the weak backscattered reflection [33, 73].

### 2.2 Self-interference mitigation

Self-interference in wireless systems occurs when a radio transmits and receives simultaneously at the same frequency. This makes it a problem particularly for full-duplex radios [7, 17, 31], where the strong transmitted signal can overwhelm the sensitive receiver. RFID readers are full-duplex in the sense that they must receive the weak backscattered signals while transmitting the unmodulated carrier in the same frequency, and thus suffer from the same issue.

The problem is exacerbated in RFID systems because the reader, when querying the tags for their IDs, must also provide energy to the (passive) tags and hence transmits a powerful carrier signal (usually 30 dBm). To mitigate self-interference, RFID readers typically employ sophisticated mechanisms to recover the weak backscattered signal. These mechanisms are usually a combination of methods that isolate the carrier using circulators, employ RF cancellation to attenuate the carrier signal on the receive chain and finally separate the interfering carrier signal from backscatter transmissions [27]. These methods increase the power consumption, complexity and cost of the reader. For example, Impinj's R2000 RFID chip consumes an additional 500 mW when its self-interference cancellation circuit is enabled [16]. Furthermore, the use of circulators comes with an insertion loss penalty that reduces the signal strength of the received signal, which in turn limits the achievable range. CRFID applications typically employ conventional RFID readers to receive backscattered transmissions.

SDR-based readers are also often used to query CRFID tags. These readers do not include any specialized hardware to reduce self-interference from the strong carrier. Instead, they resort to operating in a bistatic configuration [11] but nevertheless the achievable range is reduced to only a few meters [26, 67, 74].

Liu et al. present a design to reduce self-interference and enable full-duplex operation on ambient backscatter devices [38]. Their design achieves a range of only a few meters. Recent backscatter systems leverage the spectral mixing property of backscatter transmissions to shift the frequency of backscatter transmissions away from the carrier to reduce self-interference [22, 33, 51, 66, 71, 73]. We build upon these designs to develop an inexpensive reader for CRFID devices that achieves a high communication range.

Ma et al. [39] use non-linear elements attached to the WISP platform to reduce self-interference and achieve accurate 3D localization. While Ma et al. [39] also reduce self-interference, we target a different problem: by shifting the carrier we reduce self-interference to lower the cost of the backscatter reader and achieve the highest demonstrated range with backscatter systems.

### 2.3 Low-power readers

There have been prior attempts to develop low-cost backscatter readers. Braidio is a backscatter reader that can switch between active and passive radios depending on the energy constraints of the host device [27]. Similar to our architecture, Braidio can function as a low-cost and low-power backscatter reader, but achieves a maximum range of 1.8 m at 100 kbps. As a comparison, we achieve a significantly higher range due to three primary reasons: First,

Braidio uses passive receivers similar to the ones found on RFID tags resulting in a sensitivity of approximately −60 dBm. By contrast, the receivers employed in our architecture are narrow-band radios with a high sensitivity level (−124 dBm). Second, we separate the weak backscattered signal from the strong carrier which improves the SNR of the backscattered transmissions. Finally, we use a bistatic operation of the reader which further reduces self-interference. Another notable attempt is from Nikitin et al., who design a simple low-cost reader [43] but achieve a range of only 15 cm.

**Do we still need backscatter readers?** Recent systems demonstrate the ability to synthesise transmissions compatible with WiFi (802.11b) [33], BLE [22] and ZigBee [30, 51] while consuming μWs of power ameliorating the need for a separate reader device. These state-of-the-art systems operate in bistatic mode with the tag co-located with the carrier generator, and demonstrate a range of tens of meters. For example, Passive WiFi [33] shows that WiFi transmissions synthesised using backscatter communication can be received up to a distance of 30 m with the tag located 1 m from the carrier generator. Our architecture, under a similar setup and frequency, achieves a range of over 200 m. While the ability to communicate over tens of meters with μWs of power consumption enables novel applications such as connected implants [30], it is not sufficient for many applications that require even longer communication range.

## 2.4 Ambient backscatter systems

Ambient backscatter leverages radio signals such as TV transmissions [37] or WiFi traffic [6, 32, 73] to dispense with the need for an external reader or a device to generate the external carrier. Parks et al. demonstrate passive tag-to-tag communication using ambient TV signals [37]. They further improve on the design to enable through-the-wall operation and achieve high throughput [50]. Ambient backscatter using TV signals, however, is limited to operate only in the vicinity of TV towers where the signal is strong enough (approx. −30 dBm) with a limited range of 30 m [50].

On the other hand, some recent systems backscatter ambient WiFi signals. Kellogg et al. demonstrate the feasibility of backscattering WiFi signals and receiving on commodity smart phones [32] at a short range 2.1 m. Zhang et al. improve upon WiFi backscatter and achieve a range of 4.8 m by using frequency-shifting to reduce interference from WiFi transmissions to weak backscatter signals. Bharadia et al. demonstrate high-throughput WiFi backscatter to distances up to 5 m [6]. Their design uses extensive self-interference cancellation techniques at the receiver which makes the system both complex and expensive. HitchHike [73] enables communication with commodity WiFi radios by changing the codewords of WiFi signals and achieves a range of 54 m. WiFi backscatter systems do not require a dedicated carrier generating device. However, these systems occupy a significant portion of the license free spectrum due to the large bandwidth (22 MHz) of WiFi signals. As a comparison our architecture achieves a significantly higher range, and uses the spectrum efficiently due to narrow-bandwidth transmissions.

# 3 DESIGN

In this section, we present our architecture, the design of the backscatter reader, the tag, the mechanisms to bring frequency diversity to backscatter tags and a cost analysis of the architecture.

## 3.1 Architecture

Our architecture is depicted in Figure 1. In contrast to traditional RFID readers, the reader is split into one or more carrier generators and one or more receivers. Part of our architecture is a tag that shifts and modulates the carrier signals when backscattering it. The rest of this section describes these components.

## 3.2 Reader

### 3.2.1 *Decoupling in Frequency and Space.*

As described in Section 2, tackling self-interference is important when aiming for low cost and high range. Our architecture achieves this by decoupling in frequency and space:

We keep the carrier signal and the backscattered signal on *different frequencies*. As opposed to conventional readers, where the carrier signal and the backscattered signal overlap in frequency, we deliberately place the carrier an offset $\Delta f$ away from the frequency on which the reader listens. Modern radio transceivers can greatly attenuate signals present in the adjacent bands. For example, the CC2500 attenuates a signal present 2 MHz away from the tuned frequency by almost 50 dB (Figure 2). This separation between backscatter signal and the carrier significantly attenuates the carrier signal without using the complex techniques and components employed on existing readers.

Our architecture also *spatially decouples carrier generation from reception*. Spatial separation further reduces interference at the receiver from the carrier signal due to propagation loss [11]. On existing RFID readers the carrier generator and the receivers are usually co-located, hence have to employ complex components like circulators to reduce self-interference. Our decoupled architecture also enables us to reduce the power consumption of the receiver (see Section 5.1). Furthermore, when operating in the 2.4 GHz band, our architecture can leverage existing devices (e.g. WiFi access points or sensor nodes) as carrier generators. Using commodity devices that are part of the infrastructure as carrier generators helps improve the scalability of the system.

### 3.2.2 *Receiver.*

Designing the reader from scratch opens the design space to select the transceiver and important parameters like intermediate frequency, bandwidth and the modulation scheme.

**Transceiver.** We select commodity narrowband transceivers to receive backscatter transmissions. Such transceivers present two major advantages: *First*, they are highly configurable in that we can select both modulation scheme and bitrate. This enables us to significantly reduce the bitrate. Since the receive sensitivity improves drastically at lower bandwidth, we can therefore significantly extend the communication range. *Second*, supporting only basic link-layer functionality, without support for high layer protocol stacks like BLE or WiFi, enables maximum configurability and a clean slate-design of the reader. Most sensing applications send only small amounts of data [47]. While these applications can benefit from high bitrates, a low bitrate is not detrimental to the application's performance. To support high bitrates, we can also operate the reader at high bitrates with reduced sensitivity.

In our implementation we select the Texas Instruments CC2500 [14] radio transceiver for the 2.4 GHz ISM band, and the

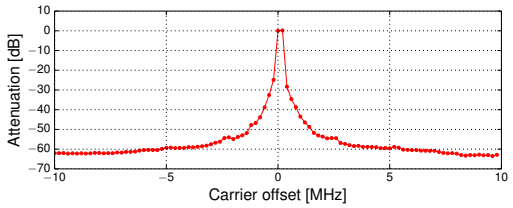


(a) CC2500 (2.4 GHz)

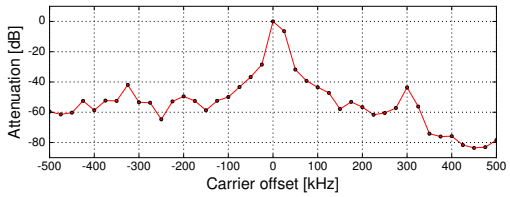


(b) CC1310 ( 868 MHz )

**Figure 2:** *Carrier interference rejection.* The transceivers reduce interference from the carrier located 2 MHz (2.4 GHz) and 100 kHz (868 MHz) away by more than 50 dB.

CC1310 [12] for the 868 MHz band because of their superior configurability, low-power and narrow bandwidth receptions.

**Intermediate frequency selection.** We use spatial and frequency separation to reduce interference from the carrier signal. The intermediate frequency $\Delta f$ for the frequency separation has to be large enough to significantly attenuate the carrier signal, leveraging the transceiver's adjacent channel rejection; but as small as possible because the tag's power consumption increases with $\Delta f$ [71].

The choice of $\Delta f$ is transceiver-dependent. We conduct experiments to determine $\Delta f$ for the transceivers we use. We set up a software defined radio (SDR) to perform a frequency sweep over a 20 MHz (2.4 GHz) and 2 MHz (868 MHz) range centered on the receiver's tuned frequency $f_c$. Meanwhile, the receiver records the received signal strength at the different carrier offsets. Figure 2 depicts the result normalized to the minimum rejection which naturally occurs at zero offset. The carrier rejection improves by almost 50 dB when the carrier is shifted 2 MHz away from $f_c$ for the CC2500. The rejection improves by 50 dB when the carrier is 100 kHz away from $f_c$ on the CC1310, without much further improvement after that. Based on these results, we consider $\Delta f$ = 2 MHz and 100 kHz as a good trade-off for the two transceivers.

**Selecting Modulation Scheme.** Since we redesign the reader from scratch, we can select the modulation scheme. The transceivers in our architecture support both On-Off Keying (OOK) and Frequency-Shift Keying (FSK).

Existing CRFID tags usually employ amplitude modulation for communication, as the passive receivers employed on these tags are often limited to amplitude demodulation using simple envelope detectors [37]. We choose FSK since it provides several advantages: *First*, FSK is a constant-envelope modulation [53] and offers robustness against fading. *Second*, FSK is more robust to noise than amplitude modulation since it can achieve a lower Bit Error Rate (BER) for the same signal-to-noise ratio [34, 53]. We employ a frequency deviation of 13 kHz and 190 kHz between the bit 0 and 1 for the CC1310 and the CC2500 respectively.

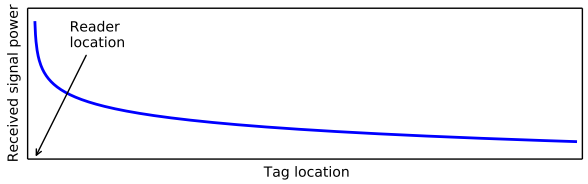


(a) Signal strength in monostatic setup, as the tag's distance to the reader increases.

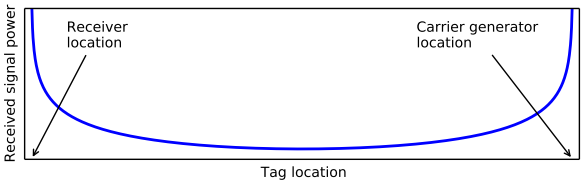


(b) Signal strength in bistatic setup, as the tag is placed on a straight line between receiver and carrier generator.

**Figure 3:** *Signal strength for monostatic and bistatic setups.* A bistatic setup increases the range, providing more locations from which the backscattered signal can be received with a high signal strength.

### 3.2.3 *Carrier Generation.*

A crucial task of our architecture is the generation of the carrier signals that are then reflected by the tags. Traditional readers delegate this task to a single device. Instead, our architecture uses a bi-static configuration and spatially separates the carrier generation and the reception. We describe this next.

**Monostatic vs. bistatic setup.** Most existing backscatter systems follow a *monostatic* setup, in which the RFID reader uses the same antenna for emitting a suitable carrier and for receiving the transmissions from the backscatter tags [34, 44]. An advantage with this setup is its conceptual simplicity. However, as discussed in Section 2, monostatic setups require the reader to perform complex interference cancellation which increases the cost and complexity.

Monostatic configurations also limit the communication range. Consider the strength $P_r$ of a backscattered signal at the reader in free space [33, 44], given by

$$P_r = \left(\frac{P_t G_t}{4\pi d_1^2}\right) K \left(\frac{\lambda^2 G_r}{4\pi d_2^2 4\pi}\right).$$

Here, $\lambda$ is the carrier's wavelength, $P_t$ is the power of the carrier, and the factor $K$ accounts for the return loss and antenna gains at the backscatter tag. $G_t$ and $G_r$ represent the antenna gain for transmitting the carrier and receiving the backscattered signal, respectively. Similarly, $d_1$ denotes the distance of the backscatter tag to the carrier generator and $d_2$ denotes the distance of the tag to the receiver. Thus, in a monostatic configuration, $d_1 = d_2$ and $G_t = G_r$. As expected, minimizing the distance to the RFID reader maximizes the received signal strength.

In contrast, our architecture uses a *bistatic* configuration, in which receiver and carrier generator do not share the same antenna and can be spatially separated. This means that for our architecture $d_1$ does not need to be identical to $d_2$. An interesting property of the bistatic configuration resulting from the duality of $d_1$ and $d_2$ is that the received signal strength is high if the backscatter tag is

located in proximity to either the receiver or the carrier generator, as we illustrate in the Figure 3.

Another advantage of the bistatic configuration is that the interference from the carrier can also be reduced due to path-loss provided that carrier generator and receiver are separated in space [11]. This further reduces the cost and complexity of the reader.

Finally, generating the carrier signal is one of the most energy consuming tasks on the reader. Co-locating the carrier generator together with reception circuitry results in a significant increase in the power consumption of the device, which makes it difficult to operate in mobile scenarios. The bistatic setup also helps achieve such capability (see Section 5.1).

**Generating carriers.** We are generally surrounded by commodity devices equipped with WiFi, BLE or ZigBee radios. Leveraging these devices to generate the carrier signal could significantly improve the scalability of our system. Interscatter [30] demonstrated that sending a special payload could help to generate short carrier signals from BLE radios. While BLE radios are very common, they are mostly found on smartphones or fitness trackers which are usually battery-powered. Delegating the energy-expensive carrier generation to devices operating on batteries might be detrimental to their life time. On the other hand, WiFi access points and ZigBee hubs are ubiquitous and are usually mains-powered, making them suitable to generate carrier signals.

To use WiFi or 802.15.4 devices to generate the carrier signal, we take advantage of the fact that most radio transceivers provide access to a special test mode that generates an unmodulated carrier signal. The radios provide this test mode to enable regulatory compliance testing. We leverage this mode to generate carrier signals from WiFi and 802.15.4 radio transceivers. In Section 4, we use TelosB sensor nodes [52] that feature a CC2420 radio chip [13], and the WiFi radio CC3200 [15] to generate an unmodulated carrier signal. Our architecture can also take advantage of the carrier signals generated by Interscatter on BLE radios. Since a carrier wave does not contain any information, the generation of carriers does not need to be coordinated in a deployment. Indeed, LoRea can use any combination of carrier generators as we show in Section 3.4.

**Carrier frequency.** Apart from using the sub GHz frequency band that conventional CRFID systems use, we primarily operate in the 2.4 GHz ISM band. A key motivation for this decision is the uniform world-wide availability of the 2.4 GHz band and its relatively high permissible transmit power. Furthermore, at 2.4 GHz our architecture can also leverage existing deployed devices like WiFi radios and sensor nodes to provide a carrier signal.

**Power consumption.** The CC3200 WiFi radio consumes 687 mW and the CC2420 802.15.4 radio consumes 54 mW to generate the carrier signal. The high power consumption required to generate the carrier signal is common to all backscatter systems [30, 33]. However, our architecture ameliorates the particular issue by enabling externally powered devices such as WiFi routers or ZigBee hubs to act as carrier generator.

## 3.3 Backscatter tag

**Design philosophy.** Existing systems, like Interscatter [30], Passive WiFi [33] or FM backscatter [68] present an IC design of the backscatter tag in a simulated environment, while the actual experiments were conducted with prototypes built using FPGAs or function generators that have a power consumption similar to low-power radios. Fabricating ICs especially in small quantities is prohibitively expensive. Our key design philosophy is to use only off-the-shelf components in the design of backscatter tag which consumes µWs of power. This brings the ultra-low power designs of backscatter tag to the wider research community immediately.

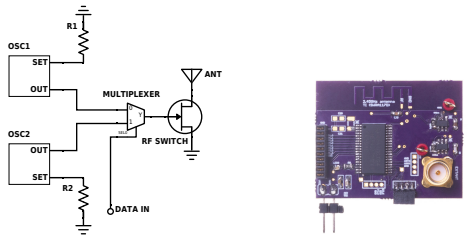


(a) Schematic (b) Prototype

**Figure 4:** *Backscatter tag schematic and prototype* The tag shifts and modulates an ambient carrier with microwatts of power.

**Backscatter tag design.** We design our tag on a two-layer FR4 PCB. We present a simplified schematic of the tag in Figure 4(a). At a high level our tag works as follows: First, using two oscillators we generate digital signals corresponding to the two frequencies (0 and 1) of the FSK signal. Next, the tag selects one of the two signals using a multiplexer chip based on the information it wants to send. Finally, the resulting signal is used to control an RF switch, which switches the antenna to reflecting or absorbing state modulating the ambient signal with the information to transmit. We show the hardware prototype of the tag in the Figure 4.

In our design, the Analog Devices HMC190BMS8 is the RF switch [25]. This switch has also been employed in recent backscatter systems [30, 33]. We select the Linear technology LTC6906 [59] and the LTC6907 [60] oscillators for the 868 MHz and 2.4 GHz tags respectively due to their ultra-low power consumption. As multiplexer, we use Analog Devices ADG904 [21].

We have measured the return loss of our tag as 3 dB, which is similar to recent designs [30, 33]. Backscatter transmissions have a side effect of creating an undesired mirror signal (see Eq. 2). Our present font-end does not remove this image. In the future, we will incorporate the design presented by Zhang et al. [73] to resolve this which might further improve the range. However, in-spite of the undesired image, owing to narrow-band transmissions, the backscatter signal, undesired mirror image and the carrier signal occupy less than 4 MHz of bandwidth at 2.4 GHz which is less than the channel spacing of 802.15.4 which eases the coexistence with other wireless networks.

For faster prototyping, we also develop a tag based on the Beaglebone Black embedded platform [9] (~ $45) and the MSP430FR5969 MCU [29] that are also used on present CRFID platforms [1].

**Power consumption.** The power consumption of the backscatter tag is dependent on both the intermediate frequency at the tag, and the operating voltage. As power consumption decreases with operating voltage [71], we operate the backscatter tag at the lowest operating voltage, which we found to be 2.1 V, the minimum required for the oscillators. To measure power consumption, we

use a highly sensitive Fluke 289 multimeter connected in series with the backscatter tag. Table 1 shows the results of these measurements. Note that the power consumption of the tag at 2.4 GHz is still an order of magnitude lower, and at 868 MHz two orders of magnitude lower, than the typical transceivers used in low-power wireless networks [13]. The higher power consumption when compared to existing state-of-the-art [30, 33, 73] is due to the use of off-shelf-components in the design of the tag. In the future, we will implement our tag on IC to reduce the power consumption.

## 3.4 Supporting frequency diversity

The ability to operate on different frequencies brings numerous advantages, for example, mitigating the harmful effects of multi-path fading, reducing interference, and improving network capacity [5]. However, state-of-the-art backscatter systems [22, 30, 33] demonstrate the ability to generate transmissions on a specific frequency. Hence, a key and unsolved challenge is to enable the ability to change the frequency of backscatter transmissions.

### 3.4.1 *Realising frequency diversity.*

To support frequency diversity, Equation 2 shows that there are two parameters that determine the channel frequency of the backscatter transmission: $\Delta f$, that is controlled by the tags, and $f_c$, that is controlled by the carrier generator. Changing the frequency at the tag has the following drawbacks:

**Tag complexity and energy consumption.** Setting the operating frequency at the tag might significantly increase the complexity of the tag's design. Both, increased complexity and larger $\Delta f$ will lead to higher energy consumption. The larger range of $\Delta f$ will further lead to an increase in the dynamic power dissipation.

**Out-of-band interference.** Large frequency shifts can also cause undesired interference even outside the intended ISM band. As discussed earlier, the backscatter tags reflect the carrier signal and shift it to the desired frequency. They, however, also shift any other transmission that occurs in the adjacent frequencies. As a result, any third-party wireless transmissions will also be shifted by $\Delta f$. We illustrate this in Figure 6 on the example of an unmodulated carrier and a WiFi transmission. The figure shows the backscatter transmissions at the desired frequency offset, but it also depicts that the WiFi transmission is shifted to the unregulated spectrum (indicated as shaded red area). Together with the above observation, we can conclude that $\Delta f$ should be kept as small as possible, which is not compatible with changing the frequency at the tag.

**Lack of carrier sensing.** One of the advantages of changing the operating frequency is to mitigate harmful effects of cross-technology interference which requires carrier sensing. However, passive receivers most commonly employed on backscatter tags are not frequency selective, and thus lack the functionality to perform carrier sensing [30]. As a result, backscatter tags are unable to decide the least interfered frequency to operate on.

*Therefore we advocate that to change the frequency of the backscatter transmissions, we change the frequency $f_c$ of the carrier signal rather than the frequency offset $\Delta f$ the tags induce when backscattering.* This keeps the backscatter tag's complexity and energy consumption low, limits out-of-band interference, and allows for informed channel selection to avoid CTI (see Section 4.4).

### 3.4.2 *Unison backscatter.*

Almost anywhere we are, we are surrounded by several commodity devices. For example, we might have sensor nodes or WiFi access points as part of the infrastructure or we carry fitness trackers that are equipped with BLE radios. Interscatter [30] demonstrated that BLE radios can generate a carrier signal and that this carrier can be backscattered as a WiFi signal at a fixed frequency. However, backscatter signals are inherently weak and are prone to interference from ambient wireless traffic. We next present a technique we call *Unison backscatter* which helps improve reliability when operating in interfered environments.

We build Unison by borrowing concepts from MIMO; receiving with multiple receivers on separate frequencies helps to improve reliability. We use several devices to generate carrier signals at different frequencies. Because of the mixing property at the backscatter tag this leads to simultaneous transmissions at all the frequencies. For example, if we have carrier signals at frequencies $f_{c1}$, $f_{c2}$ and $f_{c3}$, we get backscatter transmissions at $f_{c1} + \Delta f$, $f_{c2} + \Delta f$ and $f_{c3} + \Delta f$, respectively (assuming we discard the mirror images from the mixing operation). By having multiple receivers at the reader we can improve its reliability since it is sufficient if any of the three receivers receives the backscattered data.

While we demonstrate *Unison backscatter* for our architecture, the technique is equally applicable to other backscatter systems.

In using multiple devices to generate carrier signals, or to receive transmissions, Unison backscatter is similar to a technique presented by Zhang et al. [71]. They use multiple commodity devices to improve the SNR of the backscattered signal, while we enable concurrent transmissions on multiple frequencies at the same time. Generating carriers with multiple devices inherently increases the energy consumption for carrier generation. The devices generating the carrier are, however, usually more powerful and might also be powered externally.

## 3.5 Cost analysis

We implement our architecture using off-the-shelf components. We next present the overall cost of our architecture[1].

**Backscatter tag.** The tag is designed using Autodesk Eagle software and ordered at OSH Park [48] at a cost of 5 USD for three boards. The RF switch costs 2.5 USD, one ultra-low power oscillator costs 1.8 USD (3.6 USD for two), and the multiplexer costs 2.6 USD resulting in an overall cost of the tag around 10.3 USD.

**Reader.** We implement the 2.4 GHz reader using a CC2500 transceiver module from MikroElektronika [41] interfaced to an Arduino Zero platform [3]. The radio module costs around 20 USD and the Arduino Zero approximately 50 USD. The overall cost of the 2.4 GHz reader is hence approximately 70 USD. We implement the 868 MHz reader using a Texas Instruments CC1310 launchpad board [35] that costs around 29 USD.

**Carrier generator.** A key feature of our architecture is its ability to use wireless devices that are part of the existing infrastructure to generate the carrier signal incurring no additional cost. If needed we can also use the Texas Instruments CC3200 launchpad board (2.4 GHz) [36] or CC1310 Launchpad board (868 MHz) [35]

[1] We designed a few lab prototypes for the experiments conducted in this paper. We expect the overall cost to be substantially lower when produced at scale.

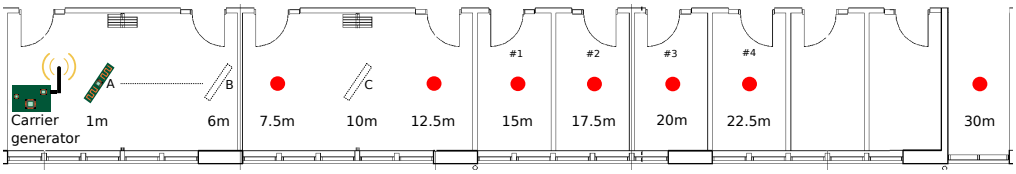


**Figure 5:** *Layout for the indoor experiments ( 2.4 GHz ).* The carrier generator is placed in the first room, while we vary the locations of the backscatter tag (A,B,C) and the receiver (red dot).

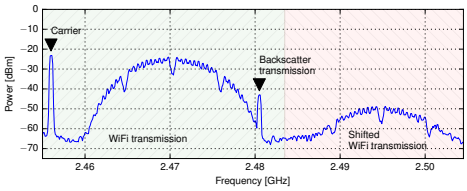


**Figure 6:** *Large frequency deviations at backscatter tag.* A large intermediate frequency at the backscatter tag also shifts ambient WiFi transmissions out of the license-free ISM band. The red shaded (\\) region is outside the unregulated band.

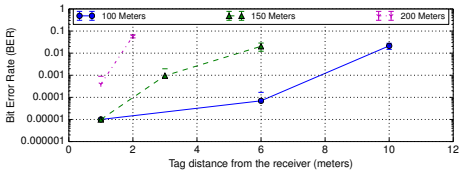


**Figure 7:** *Backscatter tag close to the receiver (outdoors, 2.4 GHz).* As the distance from the carrier generator increases, the maximum possible range between the backscatter tag and the reader decreases.

that cost around 29 USD to generate the carrier signal as we demonstrate in Section 4.2.

## 4 EVALUATION

In this section, we present experimental results to evaluate different aspects of our architecture. We perform the experiment in a range of environments and conditions. In our experiments, we find:

- In an indoor environment, with the tag co-located with the carrier source, we can communicate tens of meters even when the tag and the reader are separated by walls. When operating at 868 MHz, we can communicate through multiple floors.
- In an outdoor environment, we can communicate over distances longer than 3.4 km at 868 MHz, and 225 m at 2.4 GHz with colocated tag and carrier source, which is an order of magnitude longer than state-of-the-art backscatter systems.
- We can leverage multiple WiFi and 802.15.4 radios to provide the carrier signals at distinct frequencies to enable operations even in busy wireless environments by enabling concurrent transmissions on multiple wireless channels.
- We demonstrate that changing the frequency at the carrier generator (rather than changing the frequency offset at the backscatter tag) provides frequency diversity which increases reliability under external interference.

### 4.1 Range and Bit Error Rate

We first aim to understand the achievable range and reliability of our architecture in different environments and operating modes.

**Experimental setup.** We equip both the carrier generator and the tag with omnidirectional antennas. For experiments at 2.4 GHz we employ TP-Link [62] antennas, and at 868 MHz we use VERT900 [54] antennas. At the receiver, we use an onboard inverted-F antenna. We mitigate the non-uniform radiation pattern of the receiver onboard antenna by orienting the antenna towards the tag which improves the signal-to-noise ratio (SNR) of the received signal. To account for different antenna orientations and multi-path fading, we perform three independent runs of each experiment.

We generate a carrier signal with a strength of apporximately 26 dBm at 2.4 GHz using a USRP B200 software defined radio [4] equipped with an external amplifier. At 868 MHz, we generate a carrier of strength approximately 28 dBm using a CC1310 [12] coupled together with an amplifier. We note that the carrier signal is a few dBs lower than the maximum permissible under FCC regulation, and used by other systems [33, 73]. With a stronger carrier, we expect to improve the range. Unless otherwise stated, we position the tag, receiver and carrier generator 1 m above the ground.

**Metrics and communication parameters.** In each experiment run, we transmit 100 randomly generated packets of 64 byte and 36 byte each for experiments conducted at 2.4 GHz and 868 MHz respectively. On the receiver, we keep track of the received packet sequence number, signal strength and the noise floor. We collect approximately $10^5$ bits, and compare the received bits with the transmitted bits as done in recent backscatter works [6, 71]. We calculate the bit error rate (BER) for each run of the experiment, along with its mean and standard deviation between runs. Unless otherwise stated, the backscatter tags transmit at a rate of 2.9 kbps.

#### 4.1.1 2.4 GHz *architecture.*

**Outdoors.** We begin our evaluation outdoors with line-of-sight propagation. The experiments are conducted outside of our university, with buildings on one side and forest on the other side.

We first assess the impact of positioning the backscatter tag close to the carrier generator. Figure 8 shows the observed BER as a function of distance between the receiver and the carrier generator using the CC2500-based receiver that operates in the 2.4 GHz band. We achieve a range of 225 m, 140 m, and 90 m with a separation of 1 m, 6 m, and 12 m from the carrier generator, respectively. In most cases, the BER is well below $10^{-2}$ which is comparable to state-of-the-art backscatter systems [37, 50, 73]. As the tag moves away from the carrier generator, the achievable range decreases while the bit errors increase.

We next evaluate the impact of positioning the tag close to the reader. Figure 7 shows the result of the experiment. As both the tag and the reader move farther away from the carrier generator, the communication range decreases. When the tag is at a distance of 200 m from the carrier generator, the reader can only receive reliably

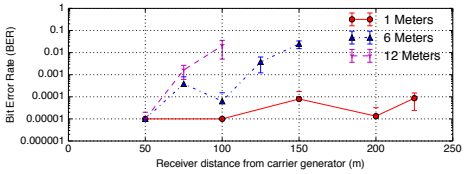


**Figure 8:** *Backscatter tag close to the carrier generator (outdoors,* 2.4 GHz*).* Positioning the backscatter tag close to the carrier generator leads to a high range. A distance of 12 m is sufficient to achieve 100 m range at a BER of $10^{-2}$.

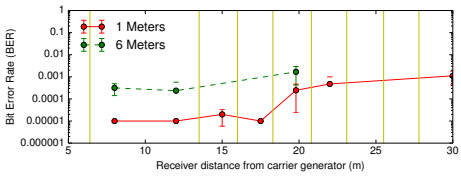


**Figure 9:** *Through the wall* (2.4 GHz). The vertical lines indicate the presence of walls. When the tag is kept 1m from the carrier generator, we can receive transmissions eight walls away at a distance 30 m from the carrier generator.

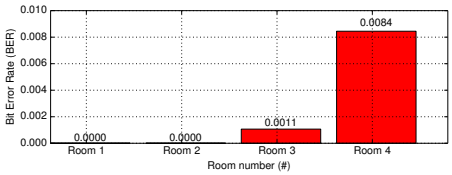


**Figure 10:** *Room to room backscatter* (2.4 GHz). Carrier generator and backscatter tag are placed in separate rooms and are separated by 10 m (tag position C). We can receive transmissions even four rooms away from the tag.

up to 2 m from the tag. However, when the distance between carrier generator and tag is 100 m, we can receive reliably even when the distance between tag and receiver is 10 m.

The results of the experiment suggest that the optimal position to achieve low BER and high range is to either position the backscatter tag close to the carrier generator, or to take the reader close to the backscatter tag, especially when operating at longer distances from the carrier generator. These results correspond to the theoretical findings in Section 3.2.3.

**Indoors.** Next, we evaluate the ability of LoRea to operate in non-line-of-sight environments. We perform experiments in an indoor environment in the presence of rich fading and other wireless networks. The environment is shown in Figure 5. The study rooms are of varying size between 2.5 m and 7.5 m, and each room is separated by an insulated gypsum wall of approximately 16 cm. The rooms are equipped with tables, chairs, and a whiteboard on the wall separating the rooms.

In a first experiment, we place the backscatter tag and the carrier generator in the same room (see Figure 5). We position the backscatter tag 1 m and 6 m away from the carrier generator. We vary the position of the receiver by placing it in different rooms.

Figure 9 shows the results, where vertical lines indicate the presence of walls in the figure. When the tag is located at a distance of

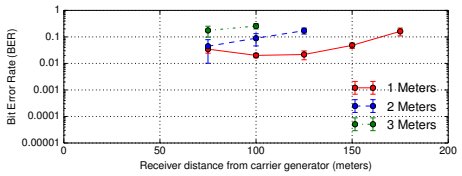


**Figure 11:** *High bitrate (197 kbps)* (2.4 GHz*, outdoors).* A High bitrate reduces the achievable range and introduces higher bit errors as opposed to operating the reader at lower bitrates. The tag was co-located with the carrier generator.

1 m from the carrier generator, we can achieve a distance of approximately 30 m between the receiver and carrier generator, traversing through eight walls. At longer distances the SNR falls below the sensitivity level of the radio. As the distance between the tag and the carrier generator increases to 6 m, the strength of the backscatter signal reduces, which affects the achieved range and also introduces higher bit errors. We achieve a range of approximately 20 m with five walls separating the tag and the receiver.

**Room to Room Backscatter.** We next evaluate LoRea in a scenario where tag, carrier generator and the receiver are all located in separate rooms. We keep the carrier generator in the same location as in the earlier experiment, and move the tag to the next room (tag position C). The distance between the tag and the carrier generator is 10 m, and a wall separates them. We place the receiver in different rooms and repeat the experiment.

Figure 10 shows the result of the experiment. We can receive backscattered transmissions four rooms away from the backscatter tag with four walls separating the backscatter tag and the receiver at a BER lower than $10^{-2}$. We note that existing CRFID systems do not operate well in through-the-wall scenarios [50]. Hence, we believe that LoRea's ability to perform well in through-the-wall scenarios is a significant improvement.

**High-speed mode.** Some sensing applications such as battery-free cameras [42] or microphones [61], suffer from the low bitrates of CRFID. To support such applications, LoRea supports higher bitrates at the cost of reduced receiver sensitivity. We next perform an experiment outdoors to investigate this trade-off. We program the reader and the receiver to operate at a bitrate of 197 *kbps* at 2.4 GHz, which is close to the maximum achievable goodput of IEEE 802.15.4 [64], a widely used protocol in wireless sensor networks.

We position the tag close to the carrier generator at distances of 1, 2 and 3 m, and place the reader at intervals of 25 m starting at a distance of 75 m from the carrier generator. Figure 11 shows the result of the experiment. While we achieve a range of 100 m at a target BER of $10^{-2}$ when the tag is located 1 m apart from carrier generator, the BER increases significantly at larger distances.

The observed BER is significantly higher than at low bitrates at similar distances. However, the BER we achieve is comparable to the recent backscatter systems operating at similar bitrates and frequency, while we get a nearly threefold improvement in range [73]. The experiment suggests that high-speed mode should only be used at short distances or together with suitable mechanisms at the reader to recover lost or corrupt bits, or to improve the reliability of links using error correction and bit spreading mechanisms as we describe in our recent work [65].

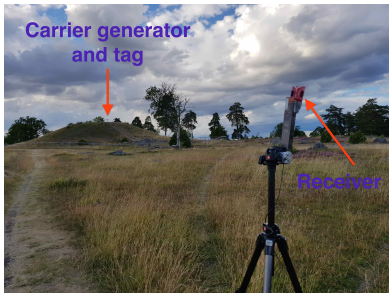


**Figure 12:** *Long distance backscatter.* Carrier generator and tag were co-located on a small plateu a few meters above the ground. The receiver was approximately 2 m above the ground on a tripod.

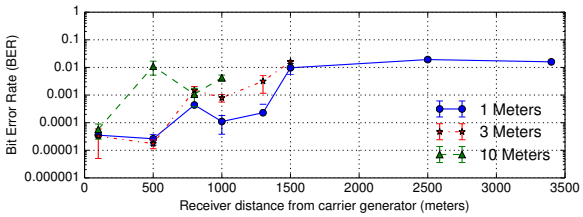


**Figure 13:** *Long range backscatter (outdoors,* 868 MHz*).* Even when the carrier generator and tag are located 10 m apart, we can communicate to distances as high as 1 km. At a distance of 1 m between tag and carrier source, we can communicate to distance of 3.4 km

*4.1.2* 868 MHz *architecture.*

LoRea when operating at 868 MHz enables higher range and preserves compatibility with existing CRFID platforms like WISP. While the focus of our work is to use 2.4 GHz which enables the use of commodity wireless devices as carrier generators, we present encouraging results the architecture achieves at 868 MHz. For brevity, we present results where the tag close is to the carrier generator, and the maximum range achieved with the tag equidistant between the carrier generator and the receiver.

**Co-located tag and carrier generator (Outdoors).** In this experiment, we investigate the maximum range achievable with our architecture in an outdoor line-of-sight environment. We perform an experiment similar to the one performed earlier at 2.4 GHz. We perform the experiment in a large open space with some trees and vegetation. We co-locate the carrier generator with the backscatter tag 1 m above ground on a small plateau of a few meters height (as shown in Figure 12). We keep the receiver on a tripod approximately 2 m above the ground. We position the backscatter tag at a distance of 1, 3 and 10 m from the carrier generator.

Figure 13 demonstrates the result of the experiment. At a distance of 1 m between carrier source and tag, we can receive transmissions 3.4 km away. At this distance the received signal strength is close to the sensitivity level of the receiver and requires orientation of the antenna to maximize the SNR. The bit error rate is still moderate around 1.5%. Similarly, we can communicate upto a maximum distance of 1.5 km and 1 km when the distance between the tag and carrier generator is 3 m and 10 m respectively. We observe slightly anomalous results at a distance of 800 m due to the presence of a large tree. To the best of our knowledge, this is the highest range demonstrated with backscatter communication and significantly advances the state of the art.

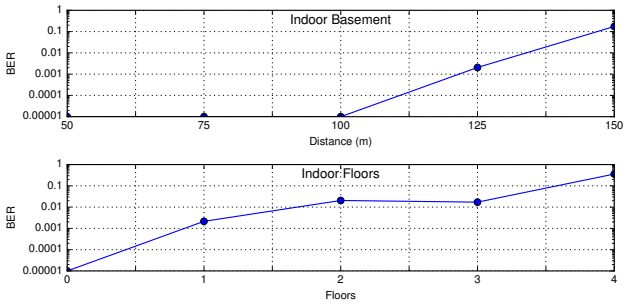


**Figure 14:** *Indoors (*868 MHz*).* We can communicate through several floors of the university building. The tag and carrier generator are separated by 1 m.

**Co-located tag and carrier generator (indoors).** We also evaluated our system in the indoor environment. We place the carrier generator and the tag separated by 1 m. As we get substantially longer range than when operating at 2.4 GHz, we perform the experiment at the basement of our university, and on different floors directly above the tag. In the basement, in most locations the tag and the receiver were not in line-of-sight.

Figure 14 shows the results of experiment. The figure shows that we can communicate over multiple floors of the building (up to the 4th floor). The BER increases sharply with the number of floors, as the SNR of the signal becomes progressively worse. We note, other backscatter systems [68, 73] also exhibit such sharp increase in BER when the distance increases. In the basement, we can reach a distance of 150 meters. To the best of our knowledge, no existing backscatter system has been able to demonstrate the ability to communicate through multiple floors in the building.

**Tag equidistant between carrier generator and receiver.** Finally, we perform the experiment with the backscatter tag equidistant between the carrier generator and the receiver. As discussed in Section 3.2.3, this configuration results in the weakest received signal strength and hence communication range.

We position the tag in line-of-sight with both the carrier generator and the receiver and find the maximum separation that achieves signal levels close to the transceiver's sensitivity level. In our experiment, we can keep the tag a maximum distance of approximately 75 m from both the carrier generator and the receiver. Our experiment suggests that our architecture when operating in monostatic mode can achieve a communication range as high as 75 m. This is because the particular configuration has similar path loss to the monostatic configuration of RFID readers, and hence represents a significant improvement over RFID readers that communicate only up to a maximum distance of 18 m (See Section 4.5).

## 4.2 Leveraging Carriers from Existing Infrastructure

**Simultaneous carrier from commodity radios.** In this experiment, we investigate the impact of generating a carrier from multiple devices at the same frequency. We deploy six MSP430-based backscatter tags in an office in close proximity to TelosB sensor nodes [52]. Their radio chips (CC2420) feature a test mode that allows to generate an unmodulated carrier at an output power of

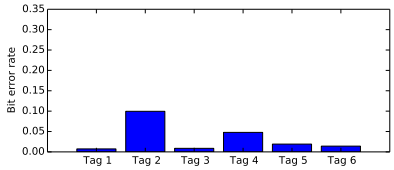


**Figure 15:** *Bit error rate for distributed-carrier setup.* LoRea can make use of several carriers from a deployed infrastructure.

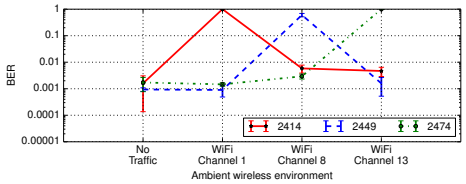


**Figure 16:** *Unison backscatter*. Leveraging multiple commodity devices to generate the carrier signal, together with multiple receivers at the reader keeps bit errors low even under external interference.

0 dBm. The tags periodically backscatter packets with random payloads. We place a CC2500-based receiver in the same room. We collect received packets over a time span of five hours.

Fig. 15 shows the BER for each of the six tags. BERs are generally low, except for tag 2, which has the longest distance to the receiver. We attribute the bit errors that we observe to interference from other coexisting wireless networks and occasional collisions between transmissions from tags. We do not observe distinct temporal variations in the bit error rate. We conclude that using several carriers simultaneously is feasible, and that slight offsets in the carrier frequency between carrier generators (which are inevitable due to variations in crystals) do not noticeably affect communication.

**Range with commodity radios.** In the next experiments, we investigate the range we can achieve when using commodity radios to generate the carrier signal. As the transmit power of these radios is much lower than those of SDRs, we expect the range to decrease. We keep the tag 1 m from the carrier generator. We perform the experiments outdoors, in line-of-sight.

First, we perform an experiment with the CC3200 WiFi transceiver. We use the CC3200 Launchpad [36] ($30) as platform. The CC3200 transmits at its maximum power of 18 dBm . We achieve a range of 54 m. We expect wireless devices such as WiFi routers that use this particular transceiver, or operate at similar output power when used as carrier generator in our architecture to result in similar range. Next, we perform an experiment with the TelosB sensor node ($70) using its 802.15.4 radio as carrier generator. The sensor node transmits at 0 dBm power. A lower carrier strength results in a maximum range of 7.5 m.

On both platforms, we only use the on-board antennas that have a limited gain which limits the achievable range. Despite the much lower carrier strength, our architecture is able to achieve a range that is comparable with the state of the art (see Table 1).

## 4.3 Unison backscatter

In this experiment, we investigate the *Unison* backscatter mechanism we developed to improve reliability under the presence of external interference. The key idea is to use several commodity devices to generate carrier signals at different frequencies that are then backscattered simultaneously to multiple receivers.

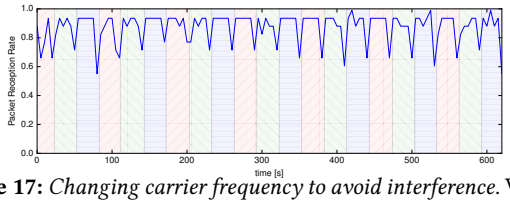


**Figure 17:** *Changing carrier frequency to avoid interference.* Vertical color bands represent the operating frequency of the backscatter transmissions. A drop in PRR corresponds to periods of interference, causing the carrier generator to change frequency improving the PRR of the received backscatter transmissions.

**Experiment setup.** We set up the experiment in our lab. We position the backscatter tag 1 m away from the carrier generators. As carrier generators, we use three CC3200 WiFi radios [15], and program them to generate carrier signals at 2412.3 GHz, 2447.3 GHz and 2472.3 GHz. We intentionally chose these frequencies as they lie within the WiFi band of the interferer. We position three receivers 8 m away from the carrier generators. To generate interference, we leverage another CC3200 radio to continuously generate WiFi traffic at maximum transmit power. We locate the interferer 6 m away from both the backscatter tag and the receivers. As in the previous experiments, we calculate the BER.

**Results.** We perform four runs of the experiment. In the first run we turn off the interferer. In the next three runs, we program the interferer to operate on WiFi channel 1, 7 and 13, respectively. Figure 16 shows the result. In the first experiment without interference, we can receive transmissions from the tag on all the three frequencies, at a very low BER. For the next three runs, the figure shows a drop in BER of the receiver whose frequency overlaps with that of the interferer. The figure shows that while there is a significant decrease in BER at the receiver that operates on a frequency similar to the interferer, the other two receivers continue to receive at low BER. We precisely enable this diversity to improve reliability when operating in interfered environments.

## 4.4 Avoiding interference

Receivers commonly employed on backscatter tags are passive envelope detectors which lack the necessary frequency selectivity to perform carrier sensing operation [30]. Carrier sensing, however, is important to ensure that backscatter transmissions do not interfere with ambient wireless traffic. To ameliorate the issue, we take advantage of the fact that carrier generators, as well as receivers, usually are much more capable devices than the tags. Receiver and carrier generators can coordinate to first identify interference, and to change carrier frequency to ensure weak backscatter transmissions avoid interference. We next demonstrate such a design:

**Setup.** We program an SDR to generate traffic imitating WiFi transmissions. We program the SDR to change the frequency corresponding to WiFi Channel 1, 7, 12 every 30 s. We keep the backscatter tag and carrier generator about 0.5 m apart and program the receiver to respond to periods with high packet error rate by sending instructions to the carrier generator to change frequency. Note that this also induces a change in the frequency of the backscatter transmission itself, to which the receiver has to adapt. To avoid interference, the carrier changes frequency when notified by the

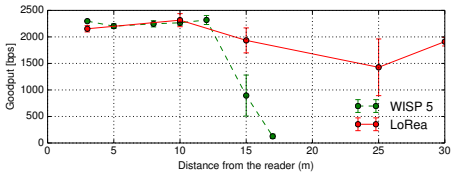


**Figure 18:** *Goodput comparison between WISP 5 and LoRea (outdoors).* WISP achieves a maximum range of only 18 meters.

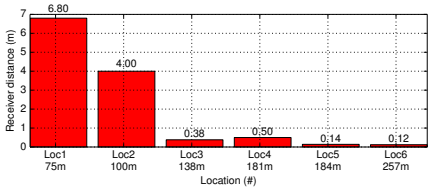


**Figure 19:** *Receiving backscatter transmissions in parking space* (2.4 GHz). The farther the tag is from the carrier generator, the closer the reader has to be to the tag to receive.

receiver. In our experiments, the carrier selects a channel that will be interfered again when the interfering SDR changes frequency.

**Result.** Figure 17 demonstrates the result of the experiment. In the figure, the bands represent distinct transmission frequencies. We observe, as soon as there is a drop in the packet reception rate (PRR) due to interference, the carrier generator changes frequency (change in color), resulting in improvement in PRR, as the backscatter transmissions are able to avoid the interfered channel.

## 4.5 Comparison with CRFID

In this experiment we compare the performance of LoRea to CRFID tags queried using a commercial RFID reader. We perform the experiment to understand improvements in terms of range.

**Settings and metrics.** We perform the experiment outdoors. We use the Wireless Identification and Sensing Platform (WISP) as CRFID platform. WISP has been widely used [1, 42, 55] and developed for close to a decade [55]. We use the present generation, and the state-of-the-art WISP 5.0 for the experiments [1]. To query the WISP tags, we use a commercial RFID reader (Impinj Speedway R420 [28], ~ $1600) equipped with a single 9 dBiC circular polarized antenna. We configure the reader to generate a carrier signal of strength 26 dBm, similar to the carrier strength used to evaluate the LoRea reader. We position the antenna and the WISP tags approximately one meter above the ground. As CRFID tags demonstrate an asymmetry in the communication and energy harvesting range [24], we externally power the WISP tags to avoid being restricted by the energy harvesting range.

In the same setting, to evaluate LoRea on 2.4 GHz, we connect a 9 dBi antenna [63] to the SDR. Due to the self-interference problem, we cannot use a monostatic setup. We emulate the equivalent path loss of monostatic configurations by keeping the carrier generator and the receiver equidistant from the tag while maximising the distance between them. We operate LoRea in low bitrate mode. We program both the WISP and LoRea to transmit with the minimum possible delay. As a metric, we measure the achieved goodput.

**Results.** Figure 18 shows that as the distance between the WISP and the RFID reader increases, the achieved bitrate drops significantly. This is due to the SNR of the backscattered signal decreasing at the reader and approaching the sensitivity level of the reader. We observe a maximum distance of approximately 17 m, which is consistent with the maximum advertised range of the Impinj Speedway R420 RFID reader [28]. Our architecture, in certain cases, achieves a range that is one order of magnitude higher as compared to existing RFID readers.

The higher range achieved by our architecture is due to three reasons. First, we shift the weak backscattered signal away from the carrier which reduces the interference, thereby improving the SNR. Second, we use a radio which offers receiver sensitivity that is almost 20 dB higher (approximately −104 dBm) compared to the −84 dBm the R420 reader offers, a typical sensitivity for commercial RFID readers. Finally, most commercial RFID readers operate in a monostatic configuration which, as we have discussed in Section 3.2.3, limits the achievable range significantly.

**Interoperability .** Our architecture, when operating at 868 MHz is compatible and can be used together with the present generation of the WISP 5.0 [1] CRFID tag with minor firmware modification to backscatter at an intermediate frequency.

# 5 PROOF-OF-CONCEPT APPLICATIONS

In this section, we present two proof-of-concept applications implemented using LoRea which are challenging to realise with existing backscatter systems.

## 5.1 Mobile Reader

Mobile backscatter readers can be useful for applications in, for example, libraries, offices, and at manufacturing lines. Existing backscatter readers, however, usually combine carrier generation with reception, making them bulky and power hungry which makes their operation difficult in mobile scenarios.

Our architecture can enable such applications, as the bistatic mode delegates the more energy-expensive tasks to the fixed infrastructure. This reduces the power consumption of the receiver. Decoupling the carrier generator, however, introduces a new challenge: tags demonstrate varied communication range, due to different distances from the carrier generator.

To demonstrate this problem, we distribute backscatter tags at six different locations in the parking space of the university. The backscatter tags are not in line-of-sight with the carrier generator. We find the maximum communication distance between the tag and the receiver. Figure 19 show that the range is longer for tags closer to the carrier generator, while for tags farther away the reader has to be close to the tag to receive transmissions.

In a concrete application scenario, one could deploy several carrier generators as shown in Section 4.2. Another option is to devise trajectories that allow the mobile reader to query the tags near the carrier generator from large distances and tags farther away from the carrier generator from short distances. While we note that our architecture enables such applications due to its low power consumption, we leave these issues to future work.

## 5.2 Sensors Embedded in the Infrastructure

Embedding sensors in the infrastructure itself is an important challenge especially for applications like structural health monitoring.

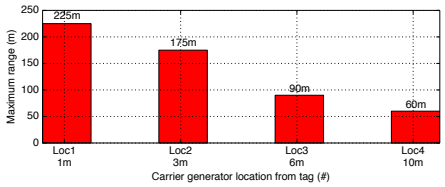


**Figure 20:** *Embedding sensor in infrastructure* (868 MHz). Even in the presence of a thick concrete wall LoRea can receive backscatter transmissions hundreds of meters away from the tag.

These sensors measure parameters like vibration, strain etc. and help improve the lifetime of the infrastructure. Making these sensors battery-free is important, as they could be embedded within the structure and left unattended for long periods of time. Existing attempts to embed CRFID sensors have resulted in very poor communication ranges (only a few meters), which severely restricts their usage in real environments [2]. Such a poor range is primarily due to the large attenuation of RF signals while going through walls, coupled with the poor sensitivity levels of RFID readers. The higher sensitivity of our receivers could enable LoRea to achieve high communication range. We explore this possibility next.

We place a tag in the basement of our building behind a thick concrete wall. Next, we place the carrier generator (868 MHz) with transmit power of 24 dBm outside such that the wall separates the two. This scenario represents the worst case scenario when compared to sensors embedded in the wall, as the backscattered signal gets attenuated twice. We find the distance up to which the receiver is able to receive transmissions, as a function of the carrier generator's distance from the tag.

The result of the experiment is shown in Figure 20. The figure shows that at a distance of 1 m between the tag and the carrier generator, we can achieve a communication range of 225 m. Even when the carrier generator is 10 m away, we still achieve a significant communication range. We believe that our architecture takes a step to make these very important applications a reality.

## 6 DISCUSSION

**Commodity wireless devices as carrier generators.** A key feature of LoRea's 2.4 GHz architecture is its ability to use existing wireless devices, such as WiFi routers and ZigBee hubs, to generate the carrier signal. On these devices, LoRea uses the *continuous carrier mode* present to facilitate regulatory compliance testing to generate the carrier signal. We performed a brief survey and found access to this mode in many commercially-available WiFi [15, 23], ZigBee [13, 40] and BLE radios [19, 45]. Devices that use these transceivers can generate a carrier signal with only a minor modification to their firmware. For example, a vast number of WiFi routers support the open source OpenWRT firmware [46]. OpenWRT enables driver-level access to the WiFi transceivers facilitating the configuration required to support the carrier generation.

**Supporting simultaneous transmissions from tags.** A crucial requirement for backscatter readers is to support simultaneous reception from multiple backscatter tags. This is particularly challenging in our architecture due to the low data rate, which increases the probability of collisions among backscatter transmissions. Conventional backscatter tags transmit at the same frequency which results in frequent collisions requiring mechanisms at the reader to separate the collided signals and recover information [26, 49]. However, such designs increase the complexity and the cost.

In our architecture, we use heterodyning at the backscatter tags to keep the carrier signal and backscatter transmissions apart reducing self-interference. Our recent work [65] demonstrates that heterodyning also enables backscatter tags to operate on distinct channels, thus enabling simultaneous transmissions without collisions. We can build upon this to support simultaneous transmissions without increasing the cost and complexity of the reader required by existing designs. Due to the limited number of available channels in the license free bands, a key challenge is to support a large number of backscatter tags . We will explore this in the future.

**Improving reliability of backscatter links.** Our architecture demonstrates reliability comparable to state-of-the-art backscatter systems [37, 50, 68, 73]. However, the BER is higher than what is usually observed in conventional wireless systems especially at larger distances between the tag and the carrier generator. We can improve reliability by building on our recent work [65] which uses bit spreading and forward error correction mechanisms to improve the reliability of FSK backscatter transmissions at low SNRs.

**Coordinating carrier generation.** The continuous generation of carrier signals can pose a problem for the coexistence with other wireless devices and may not constitute an efficient use of the spectrum. A possible solution to this problem is to coordinate the carrier generation so that carrier signals are only generated when tags should backscatter data. For example, the carrier generator can be synchronised to generate the carrier signal with the wake-up period of the backscatter tags. The design of such a coordination protocol is, however, outside the scope of this paper.

## 7 CONCLUSIONS

In this paper we have presented LoRea. LoRea departs from previous CRFID designs in that it avoids the need for complex and expensive self-interference cancellation. By decoupling carrier generation and reception, LoRea also allows to leverage existing infrastructure for generating the carrier and the use of highly sensitive narrow-band receivers. LoRea is complemented by the novel design of a backscatter tag that shifts and frequency modulates the carrier signal while consuming $\mu W s$ of power. LoRea achieves a range beyond 3.4 km when operating in the 868 MHz band, and 225 m when operating in the 2.4 GHz band which is a significant improvement over the state of the art in backscatter communication. The bistatic design of our architecture allowed to move complexity from the backscatter tag to the carrier generator and/or receiver, enabling several interesting applications as demonstrated in this paper.

## 8 ACKNOWLEDGEMENTS

We thank the anonymous reviewers and our shepherd Karthik Dantu for their insightful comments. This work has been funded by the Swedish Energy Agency (Energimyndigheten).

## REFERENCES

[1] WISP 5.0. 2017. Accessed: 02-04-2017. http://wisp5.wikispaces.com/WISP+Home. (2017).
[2] Miran Alhaideri, Michael Rushanan, Denis Foo Kune, and Kevin Fu. 2013. The Moo and Cement Shoes: Future Directions of A Practical Sense-Control-Actuate Application. (2013).

[3] Arduino Zero. 2017. Accessed: 02-09-2016. https://www.arduino.cc/en/Main/ArduinoBoardZero. (2017).
[4] Ettus Research. USRP B200. 2017. https://www.ettus.com/product/details/UB200-KIT. (2017).
[5] Paramvir Bahl, Ranveer Chandra, and John Dunagan. 2004. SSCH: Slotted seeded channel hopping for capacity improvement in IEEE 802.11 ad-hoc wireless networks. In *ACM MOBICOM 2014*.
[6] Dinesh Bharadia, Kiran Raj Joshi, Manikanta Kotaru, and Sachin Katti. 2015. BackFi: High Throughput WiFi Backscatter. In *ACM SIGCOMM 2015*.
[7] Dinesh Bharadia et al. 2014. Full Duplex MIMO Radios. In *NSDI 2014*.
[8] Naveed Anwar Bhatti et al. 2016. Energy Harvesting and Wireless Transfer in Sensor Network Applications: Concepts and Experiences. *ACM Trans. Sen. Netw.* (2016).
[9] Beaglebone black. 2017. Accessed: 01-04-2017. https://beagleboard.org. (2017).
[10] Michael Buettner, Ben Greenstein, and David Wetherall. 2011. Dewdrop: An Energy-aware Runtime for Computational RFID. In *NSDI 2011*.
[11] M. Buettner and D. Wetherall. 2011. A software radio-based UHF RFID reader for PHY/MAC experimentation. In *IEEE RFID 2011*.
[12] Texas Instruments. CC1310. 2017. Accessed: 01-04-2017. http://www.ti.com/lit/ds/symlink/cc1310.pdf. (2017).
[13] Texas Instruments. CC2420. 2017. Accessed: 01-04-2017. http://www.ti.com/lit/ds/symlink/cc2420.pdf. (2017).
[14] Texas Instruments. CC2500. 2017. Accessed: 01-04-2017. http://www.ti.com/lit/ds/symlink/cc2500.pdf. (2017).
[15] Texas Instruments. CC3200. 2017. Accessed: 01-04-2017. http://www.ti.com/lit/ds/symlink/cc3200.pdf. (2017).
[16] Impinj R2000 RFID Reader Chip. Accessed: 02-10-2016.
[17] Jung Il Choi et al. 2010. Achieving Single Channel, Full Duplex Wireless Communication. In *ACM MOBICOM 2010*.
[18] Alexei Colin and Brandon Lucia. 2016. Chain: Tasks and Channels for Reliable Intermittent Programs. In *ACM OOPSLA 2016*.
[19] Cypress Semiconductors. CYW20735. 2017. Accessed: 01-04-2017. http://www.cypress.com/file/298426/download. (2017).
[20] Arvind Deivasigamani et al. 2013. A review of passive wireless sensors for structural health monitoring. *Modern Applied Science* 7, 2 (2013), 57.
[21] Analog devices. ADG 904. 2017. http://www.analog.com/media/en/technical-documentation/data-sheets/ADG904.pdf. (2017).
[22] J. F. Ensworth and M. S. Reynolds. 2015. Every smart phone is a backscatter reader: Modulated backscatter compatibility with Bluetooth 4.0 Low Energy (BLE) devices. In *IEEE RFID 2015*.
[23] ESP8266. 2017. Accessed: 01-04-2017. (2017).
[24] Jeremy Gummeson et al. 2010. On the Limits of Effective Hybrid Micro-energy Harvesting on Mobile CRFID Sensors. In *ACM MOBISYS 2010*.
[25] Analog Devices. HMC190BMS8. 2017. http://www.analog.com/media/en/technical-documentation/data-sheets/hmc190b.pdf. (2017).
[26] Pan Hu, Pengyu Zhang, and Deepak Ganesan. 2015. Laissez-faire: Fully asymmetric backscatter communication. In *ACM SIGCOMM 2015*.
[27] Pan Hu, Pengyu Zhang, Mohammad Rostami, and Deepak Ganesan. 2016. Braidio: An Integrated Active-Passive Radio for Mobile Devices with Asymmetric Energy Budgets. In *ACM SIGCOMM 2016*.
[28] Impimj. 2016. Impinj Speedway R420. (2016).
[29] Texas Instruments. 2017. MSP430 FR5969. http://www.ti.com/product/MSP430FR5969. (2017).
[30] Vikram Iyer, Vamsi Talla, Bryce Kellogg, Shyamnath Gollakota, and Joshua Smith. 2016. Inter-Technology Backscatter: Towards Internet Connectivity for Implanted Devices. In *ACM SIGCOMM 2016*.
[31] Mayank Jain, Jung Il Choi, Taemin Kim, Dinesh Bharadia, Siddharth Seth, Kannan Srinivasan, Philip Levis, Sachin Katti, and Prasun Sinha. 2011. Practical, Real-time, Full Duplex Wireless. In *ACM MOBICOM 2011*.
[32] Bryce Kellogg, Aaron Parks, Shyamnath Gollakota, Joshua R. Smith, and David Wetherall. 2014. Wi-fi Backscatter: Internet Connectivity for RF-powered Devices. In *ACM SIGCOMM 2014*.
[33] Bryce Kellogg, Vamsi Talla, Shyamnath Gollakota, and Joshua R. Smith. 2016. Passive Wi-Fi: Bringing Low Power to Wi-Fi Transmissions. In *NSDI 2016*.
[34] J. Kimionis et al. 2014. Increased Range Bistatic Scatter Radio. *IEEE Transactions on Communications* (2014).
[35] Texas Instruments. CC1300 launchpad. 2017. Accessed: 01-04-2017. http://www.ti.com/tool/launchxl-cc1310. (2017).
[36] Texas Instruments. CC3200 launchpad. 2017. Accessed: 01-04-2017. http://www.ti.com/tool/cc3200-launchxl. (2017).
[37] Vincent Liu, Aaron Parks, Vamsi Talla, Shyamnath Gollakota, David Wetherall, and Joshua R. Smith. 2013. Ambient Backscatter: Wireless Communication out of Thin Air. In *ACM SIGCOMM 2013*.
[38] Vincent Liu, Vamsi Talla, and Shyamnath Gollakota. 2014. Enabling Instantaneous Feedback with Full-duplex Backscatter. In *ACM MOBICOM 2014*.
[39] Yunfei Ma, Xiaonan Hui, and Edwin C. Kan. 2016. 3D Real-time Indoor Localization via Broadband Nonlinear Backscatter in Passive Devices with Centimeter Precision. In *ACM MOBICOM 2016*.
[40] NXP Semiconductors. MC1319X. 2017. Accessed: 01-04-2017. http://www.nxp.com/docs/en/application-note/AN2976.pdf. (2017).
[41] MikroElektronika. 2017. Accessed: 01-04-2017. https://shop.mikroe.com/ccrf-click. (2017).
[42] S. Naderiparizi, A. N. Parks, Z. Kapetanovic, B. Ransford, and J. R. Smith. 2015. WISPCam: A battery-free RFID camera. In *IEEE RFID 2015*.
[43] Pavel V Nikitin, Shashi Ramamurthy, and Rene Martinez. 2013. Simple low cost UHF RFID reader. In *IEEE RFID 2013*.
[44] P. V. Nikitin and K. V. S. Rao. 2008. Antennas and Propagation in UHF RFID Systems. In *IEEE RFID 2018*.
[45] Nordic Semiconductors. nRF51822. 2017. Accessed: 01-04-2017. https://www.nordicsemi.com/eng/Products/Bluetooth-low-energy/nRF51822. (2017).
[46] OpenWRT. 2017. https://openwrt.org. (2017).
[47] Felix Jonathan Oppermann et al. 2014. A decade of wireless sensing applications: Survey and taxonomy. In *The Art of Wireless Sensor Networks*. Springer, 11–50.
[48] OSH Park. 2017. Accessed: 02-09-2016. https://oshpark.com. (2017).
[49] Jiajue Ou, Mo Li, and Yuanqing Zheng. 2015. Come and be served: Parallel decoding for cots rfid tags. In *ACM MOBICOM 2015*.
[50] Aaron N. Parks, Angli Liu, Shyamnath Gollakota, and Joshua R. Smith. 2014. Turbocharging Ambient Backscatter Communication. In *ACM SIGCOMM 2014*.
[51] Carlos Pérez-Penichet et al. 2016. Augmenting IoT Networks with Backscatter-enabled Passive Sensor Tags. In *ACM HOTWIRELESS 2016*.
[52] Joseph Polastre, Robert Szewczyk, and David Culler. 2005. Telos: Enabling Ultra-low Power Wireless Research. In *ACM/IEEE IPSN 2005*.
[53] Theodore S. Rappaport. 2002. *Wireless Communications: Principles and Practice* (2nd ed.). Prentice Hall.
[54] Ettus research. VERT 900. 2017. (2017).
[55] Joshua R Smith et al. 2006. A wirelessly-powered platform for sensing and computation. In *ACM UBICOMP 2016*.
[56] Vamsi Talla, Bryce Kellogg, Benjamin Ransford, Saman Naderiparizi, Shyamnath Gollakota, and Joshua R Smith. 2015. Powering the next billion devices with Wi-Fi. In *ACM CoNext 2015*.
[57] Vamsi Talla et al. 2013. Hybrid analog-digital backscatter: A new approach for battery-free sensing. In *IEEE RFID 2013*. IEEE, 74–81.
[58] Jethro Tan, Przemyslaw Pawelczak, Aaron N. Parks, and Joshua R. Smith. 2016. Wisent: Robust downstream communication and storage for computational RFIDs. In *IEEE INFOCOM 2016*.
[59] Linear technology. LTC 6906. 2017. http://cds.linear.com/docs/en/datasheet/6906fc.pdf. (2017).
[60] Linear technology. LTC 6907. 2017. http://cds.linear.com/docs/en/datasheet/6907fa.pdf. (2017).
[61] Stewart J Thomas et al. Rich-media tags: Battery-free wireless multichannel digital audio and image transmission with uhf rfid techniques. In *IEEE RFID 2013*.
[62] TP-Link. TL-ANT2408CL. 2017. (2017).
[63] TP-Link. TL-ANT2409A. 2017. (2017).
[64] Ambuj Varshney, Luca Mottola, Mats Carlsson, and Thiemo Voigt. 2015. Directional Transmissions and Receptions for High-throughput Bulk Forwarding in Wireless Sensor Networks. In *ACM SENSYS 2015*.
[65] Ambuj Varshney, Carlos-Perez Penichet, Christian Rohner, and Thiemo Voigt. 2017. Towards Wide-area Backscatter Networks. In *ACM HOTWIRELESS 2017*.
[66] Ambuj Varshney et al. 2017. Battery-free Visible Light Sensing. In *Proceedings of the 4th ACM Workshop on Visible Light Communication Systems*.
[67] Jue Wang, Haitham Hassanieh, Dina Katabi, and Piotr Indyk. 2012. Efficient and Reliable Low-power Backscatter Networks. In *ACM SIGCOMM 2012*.
[68] Anran Wang et al. 2017. FM Backscatter: Enabling Connected Cities and Smart Fabrics. In *NSDI 2017*.
[69] Daniel J Yeager et al. 2009. Neuralwisp: A wirelessly powered neural interface with 1-m range. *IEEE Transactions on Biomedical Circuits and Systems* (2009).
[70] Pengyu Zhang and Deepak Ganesan. 2014. Enabling Bit-by-bit Backscatter Communication in Severe Energy Harvesting Environments. In *NSDI 2014*.
[71] Pengyu Zhang, Mohammad Rostami, Pan Hu, and Deepak Ganesan. 2016. Enabling Practical Backscatter Communication for On-body Sensors. In *ACM SIGCOMM 2016*.
[72] Hong Zhang et al. 2011. Moo: A batteryless computational RFID and sensing platform. (2011).
[73] Pengyu Zhang et al. HitchHike: Practical Backscatter using Commodity WiFi. In *ACM SENSYS 2016*.
[74] Pengyu Zhang et al. 2014. EkhoNet: High Speed Ultra Low-power Backscatter for Next Generation Sensors. In *ACM MOBICOM 2014*.
[75] Yi Zhao and Joshua R Smith. A battery-free rfid-based indoor acoustic localization platform. In *IEEE RFID 2013*.